A stepwise route to polyploidy in yeast

Cintia Gómez-Muñoz[1,2], Nina Vittorelli[1,2,3], Maxime Gaudin[4], Nicolas Agier[1,2], Stéphane Delmas[1,2], Yann Corbeau[1,2], Marco Cosentino Lagomarsino[5,6], Gianni Liti[7], Bertrand Llorente[4] and Gilles Fischer[1,2]*

[1] Sorbonne Université, CNRS, Computational, Quantitative and Synthetic Biology, CQSB, F-75005 Paris, France.

[2] Sorbonne Université, CNRS, Inserm, Institut de Biologie Paris-Seine, IBPS, F-75005 Paris, France.

[3] Centre Interdisciplinaire de Recherche en Biologie, Collège de France, CNRS, INSERM, Paris, France.

[4] CRCM, Aix Marseille Université, CNRS, INSERM, Institut Paoli Calmettes, Marseille, France.

[5] IFOM-ETS, AIRC institute of molecular oncology, Milan, Italy.

[6] Dipartimento di Fisica, Università degli Studi di Milano, Milan, Italy and INFN sezione di Milano, Milan, Italy.

[7] IRCAN, CNRS, INSERM, Côte d'Azur University, Nice, France.

*Corresponding author

Email address: gilles.fischer@sorbonne-universite.fr

Abstract

Polyploidy is a ubiquitous biological phenomenon that promotes genetic innovation and adaptation[1]. In the budding yeast *Saccharomyces cerevisiae*, polyploid strains are widespread in natural, industrial, and clinical niches, yet their origin is unclear[2–4]. Here, we identify a novel mechanism of stepwise polyploidization that involves a Sporulate-Endoreplicate-Mate (*SEM*) sequence. We show that spore endoreplication during germination doubles the genome while preserving mating competence, enabling incremental increases in ploidy through mating with a non-endoreplicated spore from the same ascus. We experimentally demonstrate the transition from diploidy to triploidy and from triploidy to tetraploidy. Stepwise polyploidization thus positions triploids as central intermediates in ploidy evolution rather than evolutionary dead-ends. We further show that spores from intact asci can spontaneously undergo one or two successive *SEM* cycles and generate novel triploid and tetraploid strains without genetic manipulation. Natural polyploids harbor specific genomic features that are consistent with the *SEM* mechanism, including the prevalence of triploidy, extensive aneuploidy, pervasive heterozygosity, and a strong association with heterothallism[4–11]. Together, our findings establish stepwise polyploidization through iterative *SEM* cycles as the predominant natural route to polyploidy in *S. cerevisiae*.

Main

Polyploidy, defined as the presence of more than two complete sets of chromosomes, is widespread across the tree of life, with both ancient and recent polyploidization events documented in all major lineages[1]. In plants and fungi, polyploidy promotes genomic and phenotypic diversification, facilitates adaptation to stress, and contributes to ecological success and domestication[3,4,12,13]. Although less common in animals, polyploidy has played an important evolutionary role, notably through two ancient rounds of whole genome duplication (WGD) at the base of vertebrate evolution[14], and remains prevalent in fish, amphibians, and some invertebrates[15–17]. Polyploidy also arises at the tissue level in multicellular organisms[1] and is a hallmark of cancer, where it fuels genome instability, tumor evolution, and therapy resistance[18–20]. Overall, polyploidy is a powerful driver of genetic innovation and is increasingly recognized as a multifaceted force shaping evolution, adaptation, and disease[1,21].

Autopolyploidization, the increase in chromosome sets within a single species, can arise through diverse mitotic or meiotic mechanisms, including somatic cell fusion, WGD through endoreplication or cytokinesis failure, polyspermy and meiotic restitution leading to unreduced gametes[1,21,22]. Somatic genome doubling produces exclusively even ploidy states, whereas the fusion of reduced and unreduced gametes can generate triploids and other odd ploidy levels. Although triploidy has often been viewed as an evolutionary dead end due to impaired fertility, triploids can potentially serve as a bridge in the transition from diploidy to tetraploidy[21,22].

In the budding yeast *Saccharomyces cerevisiae*, between 8% and 20% of natural isolates are autopolyploid and triploids are at least as frequent as tetraploids in natural populations[6–9], a pattern that remains difficult to reconcile with the canonical yeast life-cycle[2]. Despite early reports of triploid and tetraploid isolates more than seventy years ago[23] and laboratory demonstrations that triploids can be generated through mating-based routes[24], the natural mechanism underlying triploidization in yeast remains unknown. A prevailing model posits that *S. cerevisiae* undergoes saltational transitions from diploidy to tetraploidy through WGD (Fig. 1A), a view supported by the ancestral WGD event approximately 100 million years ago[25,26] and

observations of spontaneous autotetraploidization during vegetative growth[27–29]. In this framework, triploids are viewed as transient intermediates arising from chromosome loss during the reversion of tetraploids to diploids[31–33]. However, this model does not account for the high frequency and apparent stability of triploids in natural populations[33]. An alternative possibility would be stepwise polyploidization through successive gains of chromosome sets, in which triploids arise directly from diploids through mating with haploids, rather than as derivatives of tetraploids (Fig. 1A). Although at first sight such a stepwise route appears unlikely because natural diploids do not mate and haploids exist only transiently between spore germination and mating, we show that this double challenge is circumvented by a sequence of events that we term Sporulate–Endoreplicate–Mate (*SEM*) (Fig. 1B). We demonstrate that polyploidization through iterative *SEM* sequences is the predominant natural route to polyploidy in *S. cerevisiae*, enabling stepwise transitions from diploidy to triploidy and from triploidy to tetraploidy.

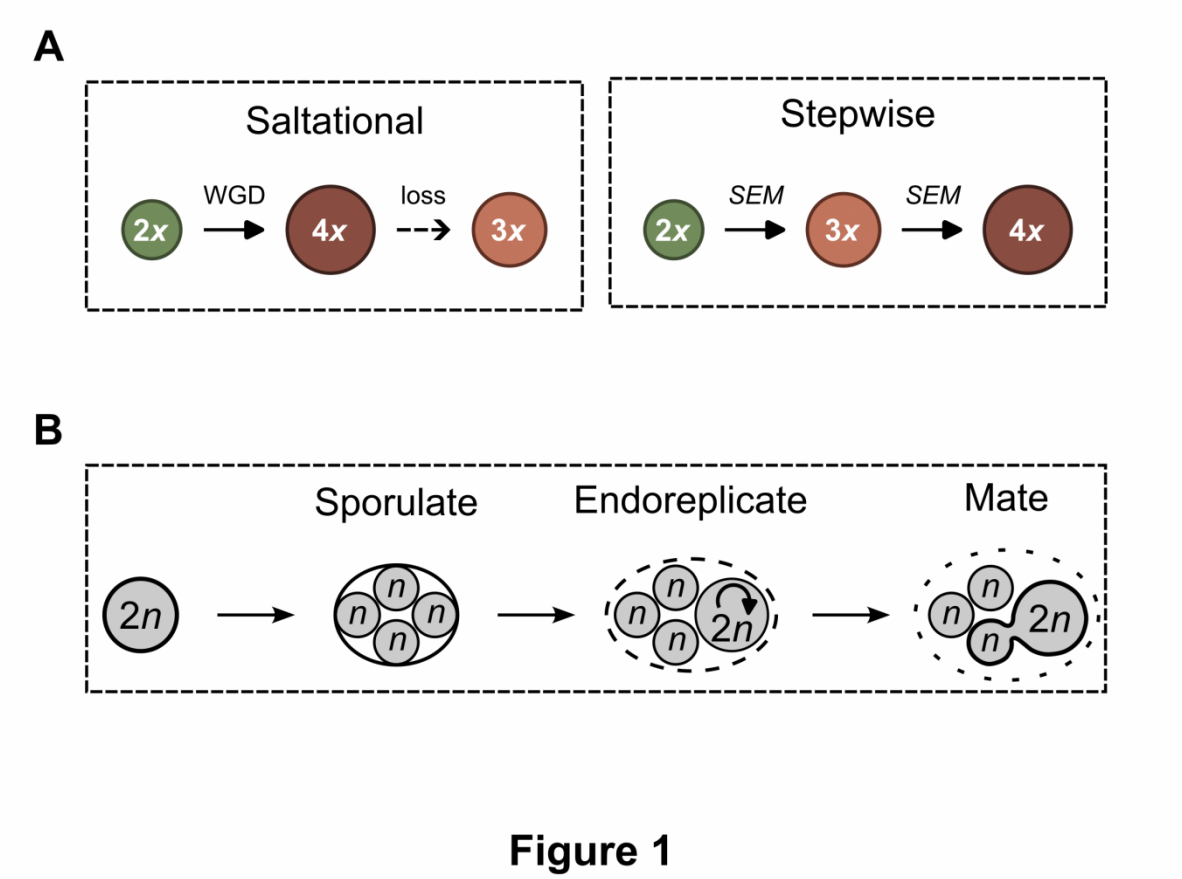

Figure 1

Figure 1: Saltational and stepwise routes to polyploidy in *S. cerevisiae*.
A, Schematic comparison between saltational and stepwise polyploidization, where x denotes ploidy level. In the saltational model, diploid cells ($2x$) undergo Whole Genome Duplication (WGD) to directly generate tetraploids ($4x$), whereas triploids ($3x$) arise secondarily through chromosome loss from tetraploids. In stepwise polyploidization, ploidy increases incrementally through successive Sporulate–Endoreplicate–Mate (*SEM*) cycles. **B**, Schematic representation of the *SEM* sequence, where $2n$ and n denote vegetative and gametic chromosome number, respectively. Sporulation of a $2n$ vegetative cell produces four $1n$ spores. Upon germination, one spore undergoes post-meiotic endoreplication, doubling the genome while preserving mating competence. Mating between the endoreplicated spore and a compatible spore from the same ascus generates a cell with increased ploidy.

The Sporulate-Endoreplicate-Mate sequence

In this study, we follow the terminology of Ramsey & Schemske[22], where $2n$ refers to the vegetative chromosome number and n to the gametic chromosome number, independently of ploidy. Ploidy levels are indicated by x, with diploids, triploids, and tetraploids corresponding to $2x$, $3x$, and $4x$, respectively.

The *SEM* sequence describes a succession of events that begins with *S*, the sporulation of a $2n$ vegetative cell which produces four $1n$ spores enclosed within an ascus (Fig 1B). This is followed by *E*, an endoreplication event that occurs upon spore germination. Here, endoreplication is used as a generic term encompassing both endocycling and endomitosis[34,35], reflecting the fact that the exact molecular mechanism underlying genome doubling is currently unknown. Endoreplication of a germinating spore generates a cell with a duplicated genome and carrying a single mating type that is thus capable of mating, while the ascus environment concomitantly supplies a compatible non-duplicatd partner. The final event is *M*, the mating between the endoreplicated spore and a compatible spore from the same ascus, resulting in a cell carrying a $+1x$ ploidy increment (Fig. 1B). Each iteration of the *SEM* sequence increases ploidy by one chromosome set (Fig. 1A).

Below, we provide experimental evidence for each step of *SEM* sequence. Additionally, we were able to experimentally recapitulate the full process of stepwise ploidy increases $2x \rightarrow 3x \rightarrow 4x$ through two iterations of the *SEM* sequence. Importantly, the stepwise polyploidization model predicts the frequent emergence of both triploids and tetraploids and suggests that increasing ploidy above $4x$ is rare. Finally, we verified that the genomic characteristics of most natural polyploids are

120 fully compatible with their stepwise origin and that the saltational route accounts
121 for a minority of cases.

122 Stepwise diploid-to-triploid transition

123 Iteration one of the *SEM* sequence starts with *S1* the sporulation of a diploid parental
124 cell and is directly followed by *E1* the endoreplication of one of the germinating
125 spores (Fig. 2A). Previous studies showed that endoreplication occurs frequently in
126 vegetative cells, with approximately 17% of haploids spontaneously diploidizing
127 after 100 generations in the absence of external stress, and can even reach 100% in
128 the presence of EtOH or KCl[36]. Endoreplicated strains are fully homozygous across
129 the entire genome, hence carry a single mating type enabling them to mate.
130 To detect endoreplication in natural populations, we screened a collection of 742
131 natural diploids using a combination of mating assays (Extended Methods) to
132 identify endoreplicated strains capable of mating but persisted without finishing the
133 *SEM* sequence. As expected, most strains exhibited no or extremely low levels of
134 mating activity. Nevertheless, a subset of strains showed clear and reproducible
135 mating signals (Table S1, Fig. 2B). We further characterized these strains by PCR
136 genotyping the *MAT* locus. We identified 26 single mating type diploids capable of
137 mating. About half of these were heterozygous at the genome level, suggesting they
138 arose through *MAT* locus hemizygotization or homozygotization (Fig. 2B). These
139 strains could contribute to polyploidization upon outcrossing, independently from
140 the *SEM* sequence. The other eleven strains were fully homozygous, indicating that
141 they most likely resulted from endoreplication (Fig. 2B). They belong to eight
142 different clades suggesting that endoreplication is pervasive across *S. cerevisiae*
143 populations (Table S1).
144 This initial screen provides clear evidence that spontaneous endoreplication occurs
145 at measurable frequencies in natural yeast populations. To determine whether
146 endoreplication can occur concomitantly with spore germination, as proposed for
147 the *E1* step of the *SEM* sequence (Fig. 2A), we screened 23 homothallic and 9
148 heterothallic diploid strains for their capacity to undergo spontaneous spore
149 endoreplication. We sporulated all 32 strains, measured the ploidy by flow
150 cytometry of 684 microdissected spores from their meiotic progeny, and determined

151 their mating genotype (Table S2, Table S3). Homothallic diploids produce haploid
152 spores that self-mate through mating-type switching, generating *MATa*/*MATα*
153 diploid monosporic isolates. As expected, all 23 homothallic diploids produced
154 exclusively *MATa*/*MATα* diploid monosporic isolates, and none showed evidence
155 of endoreplication, which would have resulted in tetraploid monosporic isolates
156 (Fig. 2C). In contrast, heterothallic diploids produce haploid spores that cannot
157 switch mating-type and therefore develop into single-mating-type haploid
158 monosporic isolates. Consistent with this expectation, all heterothallic strains
159 produced single–mating-type haploid monosporic isolates (Fig. 2C). Notably, five
160 of the nine heterothallic strains also produced ~2*x* single-mating-type monosporic
161 isolates, suggesting that endoreplication occurred after spore germination.
162 We next tested whether these putatively endoreplicated isolates were able to
163 generate triploid strains by crossing them with compatible haploid testers
164 (corresponding to the *M1* step in Fig. 2A). The ~2*x* monosporic isolates derived from
165 the two heterothallic strains AKR and ALH, both belonging to the Asian
166 fermentation clade, produced triploid progeny upon mating, confirming that these
167 isolates were endoreplicated (Supplementary Fig. 1).
168 Together, these results demonstrate that (i) a subset of natural isolates likely
169 originates from spore endoreplication, (ii) endoreplication can occur upon spore
170 germination, and (iii) endoreplicated isolates are capable of generating triploid
171 strains. These findings further reinforce the strong association between
172 heterothallism and natural polyploidy[5], as only heterothallic diploids generated
173 triploid isolates through the *SEM* pathway.

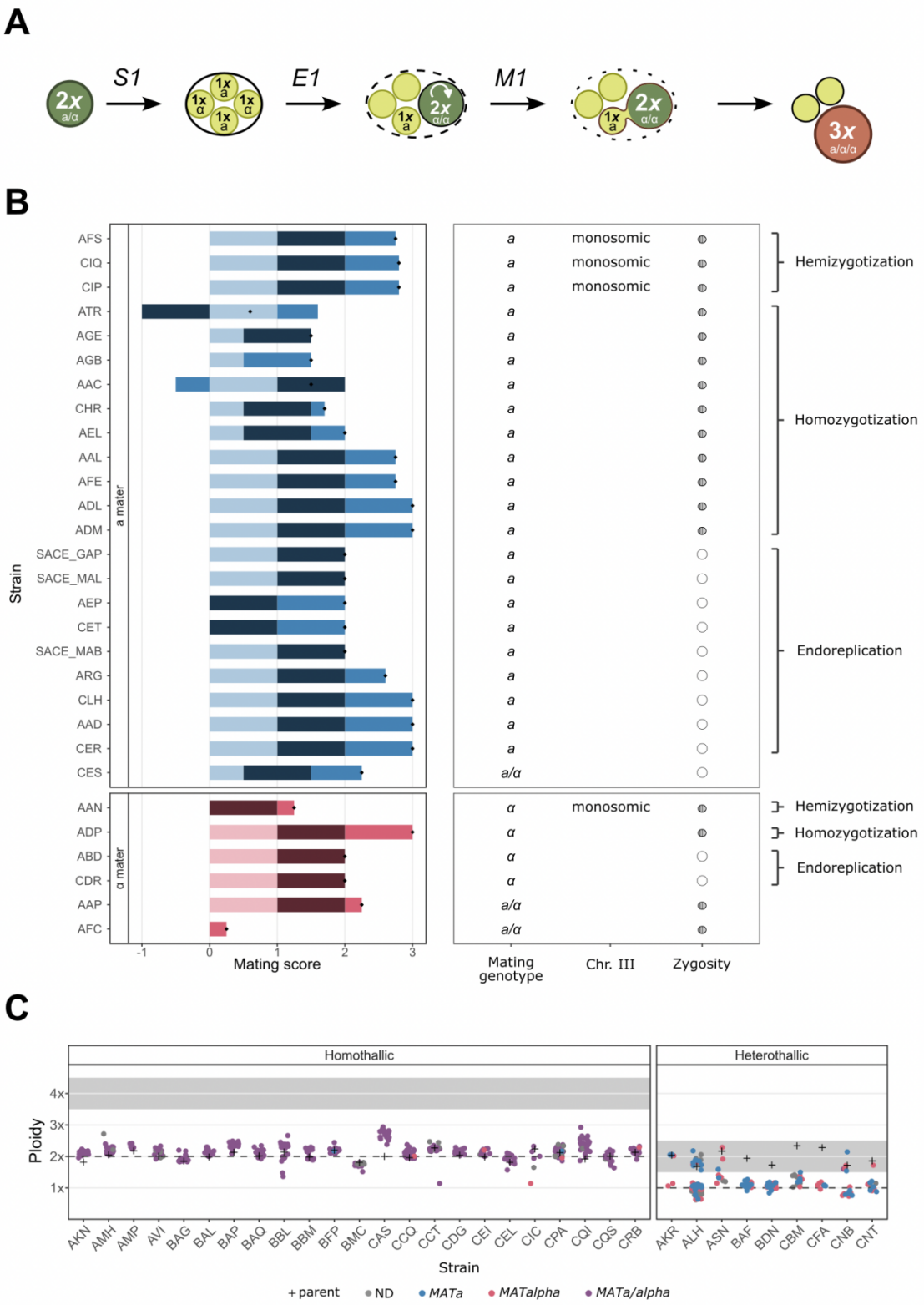
A
S1
E1
M1
2x a/α
1x a
1x α
3x a/α/α
B
Strain
a mater
α mater
AFS
CIQ
CIP
ATR
AGE
AGB
AAC
CHR
AEL
AAL
AFE
ADL
ADM
SACE_GAP
SACE_MAL
AEP
CET
SACE_MAB
ARG
CLH
AAD
CER
CES
AAN
ADP
ABD
CDR
AAP
AFC
-1
0
1
2
3
Mating score
a
monosomic
a/α
α
Mating genotype
Chr. III
Zygosity
Hemizygotization
Homozygotization
Endoreplication
C
Homothallic
Heterothallic
Ploidy
4x
3x
2x
1x
AKN
AMH
AMP
AVI
BAG
BAL
BAP
BAQ
BBL
BBM
BFP
BMC
CAS
CCQ
CCT
CDG
CEI
CEL
CIC
CPA
CQI
CQS
CRB
AKR
ALH
ASN
BAF
BDN
CBM
CFA
CNB
CNT
Strain
+ parent
ND
MATa
MATalpha
MATa/alpha

Figure 2

175 **Figure 2: Endoreplication during spore germination enables diploid-to-triploid transition**
176 **A**, Schematic of the first iteration of the *SEM* sequence, in which sporulation (*S1*), endoreplication
177 (*E1*), and mating (*M1*) collectively enable the transition from diploid to triploid. **B**, Identification of
178 natural diploid strains capable of mating. Mating scores include mass mating assays (medium
179 shading), observation of zygote formation (dark shading) and creeping phenotypes (light shading),
180 revealing a subset of diploid isolates exhibiting reproducible mating activity, as *a*-mater (blue) or *α*-
181 mater (red). *MAT* locus hemizygotization corresponds to chromosome III monosomy. Genome-wide
182 homo and heterozygosity are symbolized by open and stripped circles, respectively. Fully
183 homozygous single-mating-type diploids are inferred to result from haploid endoreplication. **C**,
184 Ploidy and mating-type composition of monosporic isolates derived from homothallic and
185 heterothallic diploid strains. Homothallic strains produce exclusively *MATa*/*MATα* diploids (purple),
186 whereas heterothallic strains generate haploid *MATa* (blue) or *MATα* (pink). Black crosses indicate
187 parental strain ploidy. The shaded area indicates the ploidy range expected from endoreplication.
188 Several heterothallic diploids produce monosporic isolates consistent with endoreplication. The
189 homothallic CAS strain produces monosporic isolates showing increased ploidy compared to the
190 parental, although lower than expected for endoreplication.

191 ## Stepwise triploid-to-tetraploid transition

192 The second iteration of the *SEM* sequence allows stepwise acquisition of tetraploidy
193 and begins with *S2*, the sporulation of a triploid parental cell (Fig. 3A). Among 46
194 triploids from the 1,011 collection, 38 (87.5%) were able to sporulate, with efficiency
195 ranging from 3% to 97% (median 44%)[37]. We microdissected 180 spores from the
196 meiotic progeny of each of three representative euploid triploid strains and
197 confirmed that spore viability was extremely low (5.0–7.8%; Supplementary Fig. 2,
198 Table S3). This could be due to chromosome missegregation or mutational load. To
199 disentangle their respective contribution, we constructed a fully homozygous
200 triploid strain (AKN-3*x*) and measured its gamete viability. This artificial triploid
201 showed 56.7% gamete viability (Supplementary Fig. 2), versus 96% in the original
202 AKN diploid strain (Table S3), indicating that segregation defects alone reduce
203 fertility by approximately 2-fold in triploids, as previously reported[38]. The even
204 lower viability of natural triploids (5.0–7.8%) highlights the additional contribution
205 of mutational load in their genomes, estimated to comprise several heterozygous
206 high-impact variants in essential genes[39].
207 Because triploid cells carry an odd number of homologs for each chromosome,
208 segregation at meiosis I is necessarily unbalanced, and triploid meiosis is therefore
209 expected to produce spores with variable chromosomal contents ranging from 1*x* to
210 3*x* (expected mean 1.5*x*, Fig. 3A). Genome sequencing of 32 monosporic isolates from

211 three natural euploid triploids showed that all spore genomes were aneuploid, *i.e.*
212 none were perfectly haploid, diploid or triploid (Fig. 3B; Table S2).
213 We identified genomic signatures of *E2*, the endoreplication step of the *SEM*
214 sequence (Fig. 3A), in six of the 32 sequenced monosporic isolates (Supplementary
215 Fig. 3). First, these isolates contain multiple chromosomes present in four copies (Fig.
216 3B). Because regular meiotic segregation of parental triploid genomes can generate
217 at most three copies of a chromosome per spore, tetrasomes are most
218 parsimoniously explained by endoreplication of originally disomic chromosomes.
219 Second, these six isolates are completely devoid of monosomes, in contrast to their
220 widespread presence in non-endoreplicated spores, suggesting that all originally
221 monosomic chromosomes were converted into disomes by endoreplication (Fig. 3B).
222 Third, allele balance ratios (*ABRs*) at heterozygous sites show ~50% heterozygosity
223 for tetrasomes and complete homozygosity for disomes in all six isolates, as
224 expected under endoreplication, although three isolates also exhibit additional *ABR*
225 complexity affecting a small number of chromosomes (Fig. 3C, Supplementary Fig.
226 3). Additionally, the six isolates exhibited ploidy levels ranging from 2.2*x* to 3.0*x*
227 (mean 2.6*x*), significantly higher than the 1.1*x* to 2.4*x* range (mean 1.7*x*) observed in
228 the other isolates (Fig. 3D). Together, these findings indicate that endoreplication
229 occurs at appreciable frequency in triploid progeny (6 of 32, 19%), supporting the
230 endoreplicate step of the second iteration of the *SEM* sequence (Fig. 3A).
231 We assessed the mating ability of the six endoreplicated monosporic isolates, along
232 with 26 non-endoreplicated isolates, by genotyping their mating types and
233 evaluating mating proficiency using mass mating assays. Five of the six isolates
234 behaved as *MATα* strains, while the remaining one was a non-mater (Table S2). To
235 validate the *M2* step of the *SEM* sequence (Fig. 3A), we crossed the five mating-
236 competent endoreplicated isolates with a haploid tester strain and measured the
237 ploidy of the resulting progeny. All crosses resulted in increased ploidy, with
238 increments ranging from +0.7*x* to +2.1*x*, demonstrating the stepwise transition from
239 triploidy to tetraploidy (Supplementary Fig. 4).
240 Together, these results show that triploid sporulation is frequent but inefficient,
241 producing few viable spores. Nonetheless, these viable progenies are highly

aneuploid, often undergo endoreplication, and can act as mating-competent partners, enabling stepwise increases in ploidy toward tetraploidy.

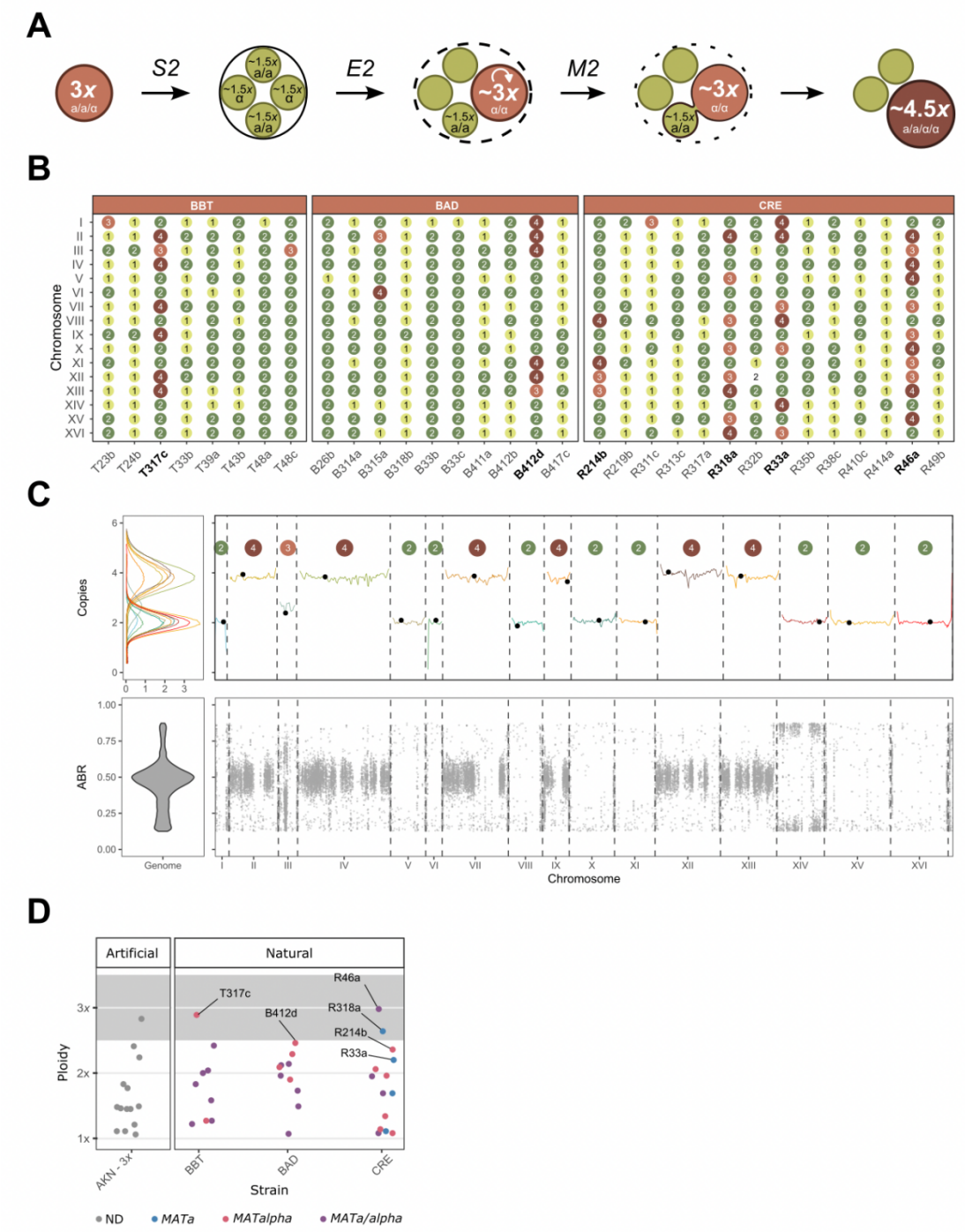

Figure 3

Figure 3: Stepwise triploid-to-tetraploid transition through the second iteration of the SEM sequence.
A, Schematic of the second *SEM* iteration (*S2–E2–M2*) initiated by sporulation of a triploid parental strain. Triploid meiosis produces highly aneuploid spores with variable chromosome copy numbers that average to 1.5*x*. The mating genotype of the parental triploid strain is *MATa*/*α*/*α*. **B**, Chromosome copy number profiles of 32 monosporic isolates derived from triploid meiosis, showing extensive aneuploidy. Six isolates (bolded names) display tetrasomic chromosomes as well as complete absence of monosomic chromosomes, indicative of post-meiotic endoreplication. **C**, Genome-wide (left) and chromosome-level (right) copy number (top) and allele balance ratio (*ABR*; bottom) profiles of the T317c monosporic isolate. Chromosome copy numbers correspond to the sequencing depth normalized by the genome ploidy. Centromeres are marked with black circles and the rounded chromosome copy number is indicated in colored circles. In *ABR* profiles, only alternative alleles are plotted. **D**, Inferred ploidy distributions of monosporic isolates, highlighting increased ploidy in endoreplicated progeny (the 6 isolates in bold in panel B are highlighted). The shaded area indicates the approximate ploidy range expected from endoreplication in monosporic isolates.

Spontaneous generation of novel polyploids through stepwise polyploidization

A key assumption of the *SEM* model is that endoreplication and mating occur sequentially and rapidly after spore germination within the same ascus. To directly test this prediction, we designed an experimental system in which diploid strains were sporulated and intact asci, *i.e.* without spore dissection, were individually micromanipulated and plated onto rich medium. This setup allowed spore germination, potential endoreplication, and intra-ascus mating to occur spontaneously under laboratory conditions, after which ascus viability was assessed and the ploidy of the resulting colonies was determined (Fig. 4A, Table S4).

We micromanipulated asci from 12 diploid strains naturally defective for mating type switching due to loss of function mutations in the *HO* gene. We focused on heterothallic strains because most natural polyploids also lack a functional *HO* gene[5], and because our results showed that only heterothallic spores endoreplicated (Fig. 2C). These strains span a broad genetic diversity, having been isolated from both natural and anthropologic niches across multiple geographic regions (Table S2). In total, we micromanipulated 1,191 intact asci (50 - 150 asci per strain). Ascus viability varied widely among strains (Fig. 4B). We recovered both haploid and diploid monoascus isolates. Haploid monoascus isolates corresponded to unmated monosporic progeny, whereas diploid isolates most likely resulted from intra-ascus mating between compatible spores (Fig. 4B). Notably, five of the twelve tested

281 diploid strains produced triploid monoascus isolates at frequencies ranging from
282 1.2% to 9.1% (Fig. 4B). In total, nine triploid isolates were recovered, subcloned, and
283 confirmed as triploid by both flow cytometry and whole-genome sequencing (Table
284 S4 and S5). Chromosome copy number and *ABR* profiles displayed values
285 characteristic of triploidy (Supplementary Fig. 6). Together, these results
286 demonstrate that sporulation of a heterothallic diploid strain can spontaneously
287 generate novel triploid progeny through at least one complete iteration of the *SEM*
288 sequence (Fig. 2A).
289 We next tested whether these newly formed triploids could undergo a second
290 iteration of the *SEM* sequence and spontaneously generate tetraploid progeny. A
291 randomly selected novel triploid isolate from each of two genetic backgrounds
292 (ALH and CNT) was resporulated. In both cases, ascus viability was reduced
293 relative to the diploid parent, consistent with impaired triploid meiosis (Fig. 4C).
294 The resulting monoascus isolates displayed a range of ploidies, including haploid
295 and diploid isolates, indicating that ploidy often regressed through meiosis as
296 expected. However, other isolates were triploid, suggesting that ploidy was restored
297 through sporulation followed by mating within the same ascus (Fig. 4C).
298 Importantly, the triploid isolates generated in this process carry novel allelic
299 combinations relative to their parental genotypes and potentially altered aneuploidy
300 landscapes resulting from meiotic resegregation of trivalents. Thus, even without
301 further increase in ploidy, these isolates enable exploration of novel genotypic space.
302 Notably, among the ascus progeny of ALH-3*x*, we identified a tetraploid isolate
303 (ALH-4*x*; Fig. 4C). This isolate was subcloned, and its ploidy was validated by both
304 flow cytometry and whole-genome sequencing (Fig. 4D and E). Comparison of
305 chromosome *ABR* profiles between ALH-3*x* and ALH-4*x* revealed the expected +1*x*
306 increase in genome content, providing direct evidence that ploidy can further
307 increase through a second iteration of the SEM sequence (Fig. 3A).
308 Together, these results demonstrate that the entire ploidy transition, from diploid to
309 tetraploid through intermediate triploid states, can be fully recapitulated under
310 laboratory conditions and harnessed to generate polyploids with novel genetic
311 compositions.

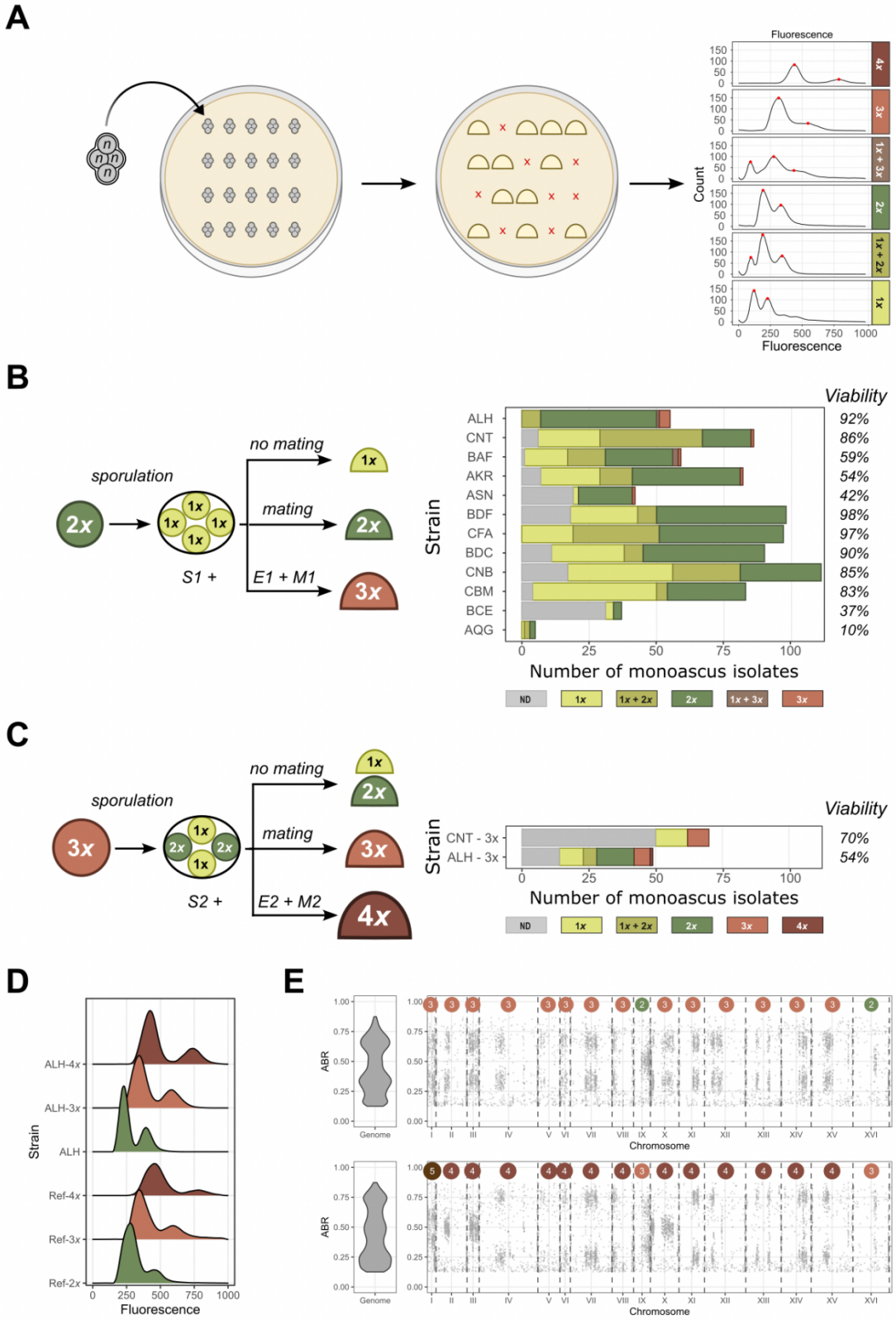
A
Fluorescence
Count
4x
3x
1x + 3x
2x
1x + 2x
1x
Fluorescence
B
sporulation
2x
1x
S1 +
no mating
mating
E1 + M1
Viability
Strain
ALH 92%
CNT 86%
BAF 59%
AKR 54%
ASN 42%
BDF 98%
CFA 97%
BDC 90%
CNB 85%
CBM 83%
BCE 37%
AQG 10%
Number of monoascus isolates
ND
1x
1x + 2x
2x
1x + 3x
3x
C
sporulation
3x
2x
S2 +
no mating
mating
E2 + M2
4x
Viability
CNT - 3x 70%
ALH - 3x 54%
Number of monoascus isolates
D
Strain
ALH-4x
ALH-3x
ALH
Ref-4x
Ref-3x
Ref-2x
Fluorescence
E
ABR
Genome
Chromosome

Figure 4

313 **Figure 4 | Spontaneous generation of novel polyploids through iterative *SEM* cycles.**
314 **A**, Experimental design for intact ascus micromanipulation, allowing spore germination,
315 endoreplication, and intra-ascus mating to occur without spore dissection. Viable asci form colonies
316 whose ploidy is determined by flow cytometry. Histograms on the right correspond to DNA content
317 measurements from representative colonies, and are not schematic. **B**, Ploidy outcomes of monoascus
318 isolates derived from heterothallic diploid strains. Triploid isolates (3*x*) arise spontaneously in
319 multiple genetic backgrounds, consistent with completion of the first *SEM* iteration. In some cases,
320 monoascus isolates exhibited mixed ploidies within the colony, with haploid and diploid, or haploid
321 and triploid cells coexisting within the same colony (1*x*+2*x* or 1*x*+3*x*). In other instances, ploidy could
322 not be reliably determined (ND) due to slow growth or multicellular clumping, a phenotype
323 frequently observed in wild strains[40]. **C**, Resporulation of newly formed triploids generates a
324 spectrum of ploidy outcomes (identical to B), including tetraploidy (4*x*), demonstrating completion
325 of the second *SEM* iteration. **D**, DNA content of ALH, ALH-2*x* and ALH-3*x* measured by cytometry.
326 The reference strains used to calibrate ploidy are the laboratory strain BY4743 (2*x*), the natural triploid
327 CRE (3*x*) and the artificial tetraploid AKN-4*x*. **E**, Genome-wide (left) and chromosome-level (right)
328 allele balance ratio (*ABR)* profiles for ALH-3*x* (top) and ALH-4*x* (bottom). Chromosome copy
329 numbers corresponding to the sequencing depth normalized by the genome ploidy are indicated in
330 colored circles.

331 A barrier to increase ploidy beyond tetraploidy

332 We explored whether further stepwise ploidy increase beyond tetraploidy was
333 achievable through the *SEM* sequence. We found that 25 of 38 (65.8%) tetraploids
334 efficiently sporulate as 25 of 38 (65.8%) were able to sporulate, with a median
335 efficiency of 57%[37]. Using two representative strains, we confirmed the low spore
336 viability of tetraploids (6.7% to 12.2%, Supplementary Fig. 2). We constructed an
337 artificial homozygous tetraploid (AKN-4*x*) to estimate gamete viability in the
338 absence of deleterious recessive mutations. This strain showed 77.2% spore viability,
339 significantly higher than the 56.7% in the homozygous triploid AKN-3*x*
340 (Supplementary Fig. 2), showing that chromosome segregation is less affected in
341 tetraploid than in triploids, as previously reported[41]. Consistently, genome
342 sequencing of 28 monosporic isolates obtained in the meiotic progeny of two natural
343 euploid tetraploids revealed very few monosmic chromosomes as well as a much
344 lower global incidence of aneuploidies than in triploid progenies (Supplementary
345 Fig. 5A). Eleven isolates were euploid diploids while the remaining showed either
346 monosomies (in seven cases) and/or trisomies (in 14 cases). Thus, the low spore
347 viability of tetraploids probably reflects the major contribution of recessive
348 mutational load exposed at homo- or hemizygous state in the gametes. No sign of
349 spore endoreplication was detected in the progeny of tetraploids, suggesting that

350 further ploidy increase through the *SEM* sequence is limited, or at least less frequent
351 than in the progeny of triploids (Supplementary Fig. 5B). Monosporic isolates
352 displayed various mating-type combinations associated with complex mating
353 phenotypes (Supplementary Fig. 5B and 5C, Table S3), including bisexual mating[42]
354 and dioecy[43].
355 Finally, genome sequencing of 16 monosporic isolates obtained in the meiotic
356 progeny of one natural pentaploid revealed consistent segregation of disomes and
357 trisomes across all isolates (a single case of monosomic chromosome I was observed,
358 Supplementary Fig. 5A). No sign of spore endoreplication was detected in the
359 progeny of the pentaploid strain.
360 In conclusion, we found no evidence supporting stepwise ploidy increase beyond
361 tetraploidy, suggesting that 4*x* might represent an upper limit for this process. This
362 is consistent with the rarity of natural pentaploids, which encompass only about
363 0.2% of strains in the largest available collection[9], and with the absence of hexaploid
364 or higher-ploidy isolates.

365 Stepwise polyploidization as the main route to natural polyploidy

366 The stepwise and saltational routes to polyploidization rely on distinct mechanisms,
367 namely the *SEM* sequence and the WGD, respectively (Fig. 1), and are therefore
368 expected to leave contrasting genomic signatures. To discriminate between these
369 modes of origin, we analyzed the genomic constitution of the 91 natural polyploids
370 from the 1,011 collection[7] and assessed whether their features are more consistent
371 with a stepwise or a saltational process.
372 We first measured the DNA content of the 91 natural polyploids by flow cytometry
373 and inferred ploidy without rounding to integer values. Rather than forming
374 discrete clusters corresponding to strict 3*x*, 4*x*, or 5*x* ploidy levels, the data revealed
375 an almost continuous ploidy range from 2.5*x* to 5.5*x* (Fig. 5A, Table S6), with clear
376 discontinuities near 3.5*x* and 4.5*x* delimiting triploid, tetraploid, and pentaploid
377 classes. Independent analysis of genome-wide *ABRs* at heterozygous sites yielded
378 ploidy estimates largely concordant with DNA content, with only three exceptions
379 (ASA, BEM, and CBR; Fig. 5A). This integrated reassessment led us to reclassify two
380 previously reported tetraploids (AFT and CFS) as triploids and to resolve one

381 previously ambiguous strain (AEC) as a tetraploid, resulting in a final dataset
382 comprising 48 triploids, 38 tetraploids, and 5 pentaploids (Table S6).
383 Under a saltational polyploidization model, the prevalence of triploids would
384 require chromosome loss from tetraploids to occur more frequently than WGD from
385 diploids. Although rapid chromosome loss has been documented in laboratory
386 engineered homozygous tetraploids[30–32], it typically results in diploid rather than
387 triploid genomes[3]. Moreover, long term vegetative propagation of natural
388 tetraploids revealed no reduction in ploidy, indicating that polyploid levels are
389 stable in natural isolates[33]. Together, these observations argue against a dominant
390 saltational origin and instead support a stepwise route to polyploidization. This
391 conclusion is further reinforced by the strong enrichment of heterothallic strains
392 among natural polyploids[5], which is expected under the *SEM* model given that
393 endoreplication is restricted to heterothallic spores (Fig. 2C).
394 Additional genomic features are likewise inconsistent with a WGD-based origin. If
395 WGD is independent from zyogosity, a saltational model predicts that the fraction
396 of homozygous polyploids should be comparable to that observed among diploids
397 (47% in the 1,011 collection[7]). In contrast, we detected only two homozygous
398 triploids and no homozygous tetraploids among the 91 natural polyploids.
399 Furthermore, WGD of a heterozygous diploid genome would produce tetraploids
400 characterized by a dominant *ABR* peak near 0.5 (Supplementary Fig. 7), a signature
401 that is never observed in our data (Fig. 5B), providing strong evidence against WGD
402 as the primary mechanism of tetraploidization.
403 Finally, combining chromosome-specific sequencing coverage with *ABRs* revealed
404 extensive aneuploidy among natural polyploids, including 122 whole-chromosome
405 and 63 segmental aneuploidies (Table S6, Fig. 5C). Under the *SEM* model, such
406 aneuploidy is expected to accumulate with increasing ploidy, as tetraploids and
407 pentaploids originate from highly aneuploid spores produced by triploid meiosis.
408 In contrast, a saltational route predicts higher aneuploidy levels in triploids arising
409 from chromosome loss in tetraploids. Consistent with the stepwise model, we
410 observed a monotonic increase in the proportion of aneuploid strains with ploidy,
411 from 52% in triploids to 78% in tetraploids and 100% in pentaploids.

412 Together, these complementary genomic signatures indicate that higher ploidy
413 levels in *S. cerevisiae* arise predominantly through iterative cycles of the *SEM*
414 sequence rather than through saltational whole-genome duplication, establishing
415 stepwise polyploidization as the main evolutionary route to natural polyploidy.

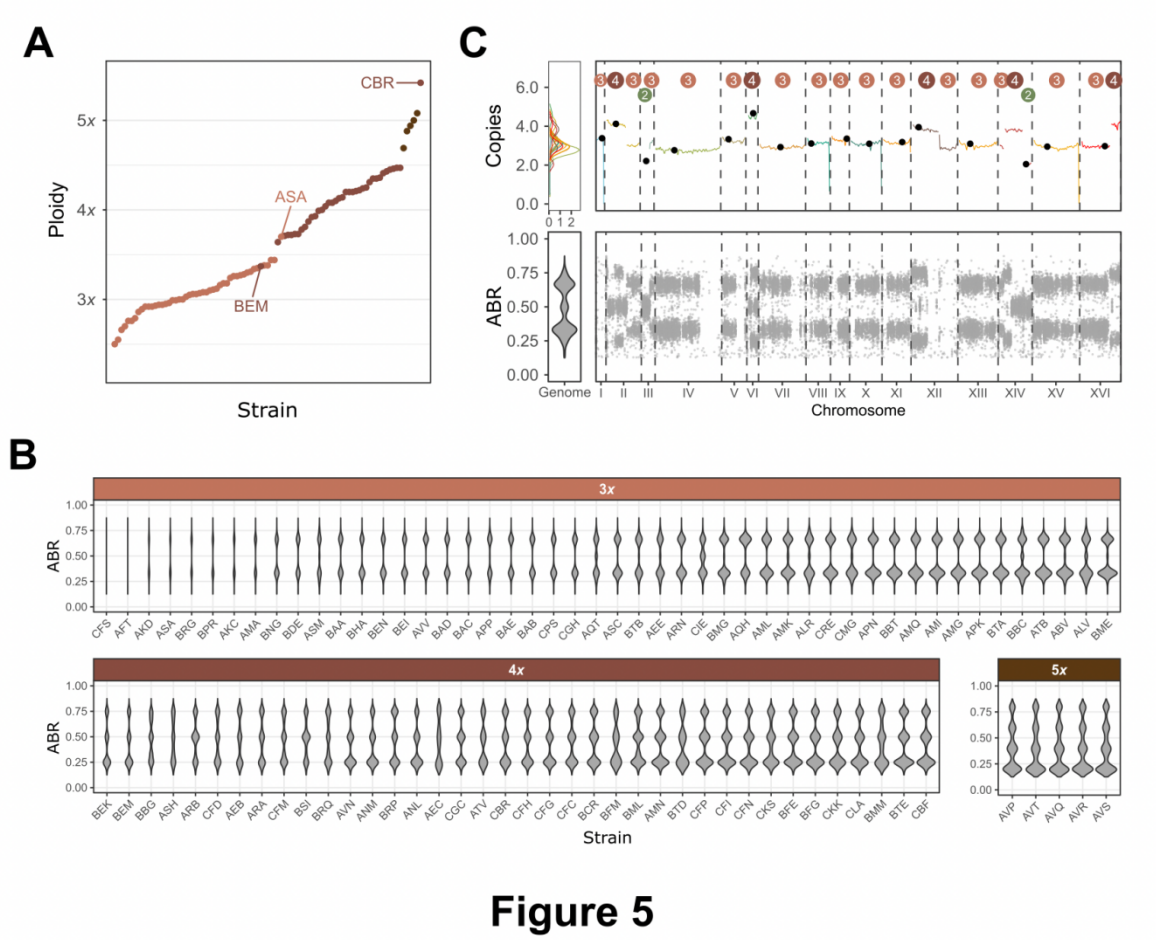

Figure 5

416

417 **Figure 5 | Genomic signatures of natural polyploids support a stepwise origin.**
418 **A**, Ploidy estimates of 91 natural polyploid isolates inferred from flow cytometry, showing a near-
419 continuous distribution from ~2.5*x* to ~5.5*x* with discontinuities delineating triploid, tetraploid, and
420 pentaploid classes. **B**, Genome-wide allele balance ratio (*ABR*) distributions for the 91 natural
421 polyploids. Observed *ABR* patterns are inconsistent with whole-genome duplication of heterozygous
422 diploids and instead support stepwise ploidy increase. **C**, Chromosome copy number and *ABR*
423 profiles of a representative natural polyploid strain (AQT) presenting several whole-chromosome
424 and segmental aneuploidies.

Discussion

Here, we identify a natural route to polyploidization in yeast that we term stepwise polyploidization, mediated by iterative cycles of the *SEM* sequence. This route begins with sporulation, followed by post-meiotic endoreplication during spore germination. The sequence ends with mating between the endoreplicated spore and a compatible meiotic product within the ascus. This process contrasts sharply with the somatic WGD in diploids, which is often invoked to explain polyploid formation in yeast, as well as with the dominant mechanism described in plants, which relies on the fusion of unreduced gametes produced by meiotic restitution[22]. Notably, a conceptually related process has been proposed in plants, where a subset of 2*x* nuclei in mature pollen may arise from mitotic endoreplication after completion of meiosis rather than from meiotic restitution[44]. This conceptual parallel suggests that post-meiotic endoreplication may contribute to polyploid formation beyond fungi.

The *SEM* model provides a unified explanation for several genomic characteristics of natural yeast polyploids, including strong association with heterothallism, pervasive heterozygosity, frequent triploid state and extensive aneuploidy. In a recent work, we showed that natural polyploidy in yeast was strongly associated with repeated losses of self-fertility[5], yet the causal basis of this association remained unclear. Our results provide a mechanistic explanation: only heterothallic spores experience a prolonged single–mating-type state upon germination that permits endoreplication, whereas homothallic spores rapidly self-mate and therefore do not enter the *SEM* pathway. At the same time, ploidy increases through mating between genetically distinct meiotic products preserve heterozygosity and account for the observed allele-balance distributions, in contrast to duplication of a single diploid genome. Stepwise polyploidization further implies that triploids are not rare anomalies but expected and stable intermediates produced by a single iteration of the *SEM* sequence. Because meiosis in triploids is intrinsically unbalanced, viable progeny are highly aneuploid, providing a direct explanation for the extensive aneuploidy observed in tetraploids. Given the broad ploidy range of spores produced by triploid meiosis, pentaploids could theoretically be generated by mating between an endoreplicated ~3*x* spore and a near-diploid partner.

456 The endoreplication step itself emerges as the pivotal mechanism of stepwise
457 polyploidization. Although the precise molecular mechanisms underlying
458 spontaneous spore endoreplication remain to be elucidated, an early study
459 identified a mutation in *CDC31*, a gene required for spindle pole body duplication,
460 as a driver of endoreduplication[45]. To date, at least 16 genes have been implicated in
461 ploidy increase in *S. cerevisiae*[46]. These genes encode proteins that primarily regulate
462 spindle pole body duplication, chromosome segregation, cytokinesis and cell-cycle
463 control, thereby highlighting the central role of cell-division and genome-
464 partitioning pathways in the control of ploidy. Moreover, high rate of
465 endoreplication depends on the presence of a functional copy of *SSD1*, a gene that
466 also regulates aneuploidy tolerance in wild yeast[47,48]. Future work will be required
467 to assess the extent of natural variation in these genes across populations and to
468 dissect the molecular events governing genome doubling associated with spore
469 germination.
470 In conclusion, our findings demonstrate that stepwise polyploidization through
471 iterative cycles of the *SEM* sequence constitutes the predominant route to natural
472 polyploidy in *S. cerevisiae*, although alternative routes, such as those involving
473 mating-competent diploids arising from *MAT* hemi- or homozygotization, may also
474 contribute. Beyond its evolutionary significance, the *SEM* mechanism has practical
475 implications. Polyploid yeast strains are widely used in fermentation industries,
476 including brewing and baking, and are also frequently isolated from clinical
477 settings[4,7–11]. The identification of the natural mechanism underlying their formation,
478 together with our ability to experimentally recapitulate *SEM*-mediated
479 polyploidization under laboratory conditions without genetic modification, opens
480 new avenues for the rational generation of novel polyploid strains. We envision that
481 controlled and potentially automated implementation of the *SEM* sequence could
482 enable the production of large numbers of polyploids with unprecedented genetic
483 compositions, offering a powerful platform for strain improvement for diverse
484 applications in the food production and fermentation industries.

485 ## Methods

486 **Strains**

487 Natural parental diploid (Table S1) and polyploid (Table S5) strains analyzed in this
488 study were obtained from the 1,011 *S. cerevisiae* collection[7] and are referred to using
489 the standardized three-letter strain code. Artificial homozygous polyploids derived
490 from the AKN (YPS128) background, as well as heterozygous polyploids derived
491 from AKN and SACE_YBP (YJM1248) backgrounds (YPB012, YPB022, YPB021),
492 were constructed as described previously[49]. Standard reference strains used for
493 ploidy calibration were as previously described[50]. Tester strains used for mass
494 mating assays were OS104a and OS104α (YPS128 background)[51].

495 **Media composition and growth conditions**

496 Standard growth medium was YPD, consisting of yeast extract (10 g L^{-1}), peptone
497 (20 g L^{-1}), and dextrose (20 g L^{-1}), prepared with or without agar (20 g L^{-1}).
498 Sporulation medium was potassium acetate (KAc) agar, containing potassium
499 acetate (20 g L^{-1}) and agar (25 g L^{-1}). Selective synthetic complete media were
500 prepared using yeast nitrogen base without ammonium sulfate (YNB; 1.7 g L^{-1}),
501 arginine (2 g L^{-1}), glucose (20 g L^{-1}), and agar (20 g L^{-1}), supplemented with
502 appropriate complete supplement mixtures (CSM). CSM + G418 medium contained
503 standard CSM and was supplemented with Geneticin (G418; 200 μg mL^{-1}). CSM -
504 Ura medium contained CSM lacking uracil (CSM - Ura). CSM - Ura + G418 medium
505 was identical to CSM - Ura and additionally supplemented with G418 (200 μg mL^{-}
506 ^{1}).

507 Unless otherwise stated, yeast cells were revived from glycerol stocks on YPD agar
508 and grown at 30 °C until the formation of a visible patch prior to experimental
509 assays. Qualitative sporulation and resporulation capacity were assessed by
510 transferring cells to KAc agar and incubating them at 30 °C. After 7 days, cultures
511 were examined by light microscopy for the presence of asci.

512 **Flow cytometry**

513 Cellular ploidy was estimated by propidium iodide staining followed by flow
514 cytometry. Ploidy validations were performed as previously described[50], using
515 cultures grown in YPD. Rapid ploidy assessments were conducted either from

516 overnight 1 mL YPD microcultures or by direct fixation of colonies in 70% ethanol.
517 Flow cytometry data were gated using FSC-A versus SSC-A and FSC-A versus FSC-
518 H to exclude debris and doublets, followed by FSC-A versus PI fluorescence
519 intensity. When required, cell aggregation was reduced by proteinase K treatment.
520 Ploidy values were inferred using MuPETFlow[50] (see Extended Methods).

521 **Genotyping mating type loci**

522 Mating genotype was determined by colony PCR as previously described[5]. In a
523 limited number of cases, PCR reactions were performed or repeated using *MAT*
524 locus primers described in[52] to confirm mating genotype assignments.

525 **Mass mating assay**

526 Query and tester cells were mixed on YPD agar and incubated at 30 °C for 24 h to
527 allow mating. Parental query cells were then streaked onto single-selection medium
528 to confirm marker compatibility, while cells from the mating patch were plated onto
529 double-selection medium to assess mating ability (see Media composition and
530 growth conditions).

531 **Multi-test screening to detect diploid maters**

532 All 742 query strains were initially tested using the mass mating assay with minor
533 modifications, and mating outcomes were scored semi-quantitatively, considering
534 as positive only the crosses that formed a confluent cellular layer (see Extended
535 Methods). A subset of 102 strains was further characterized by microscopic
536 examination of zygote formation after 4 h of co-incubation with tester strains, and
537 by assessment of creeping behavior as previously described[53] (see Extended
538 Methods). Results from the three assays were integrated into a single composite
539 mating score, and strains with a score greater than 0 were classified as potential
540 maters. Mating efficiency of candidate strains was then evaluated using a
541 quantitative mating assay adapted from[54]. Briefly, equal numbers of query and tester
542 cells (2.5×10^8 cells of each) were mixed and spotted onto a nitrocellulose filter
543 placed on YPD agar. After 4 h of co-incubation at 30 °C, cells were recovered from
544 the filter, serially diluted, and plated onto selective media to quantify colony-
545 forming units (CFUs).

546 Candidate diploid mater strains were subsequently subjected to supplementary
547 analyses to further characterize their mating behavior and genetic features. Mating
548 genotype was determined as described in the section Genotyping mating type loci,
549 and chromosome III aneuploidies and zygosity were retrieved from the original
550 sequencing data[7].

551 **Asci dissection and spore isolation**

552 Sporulated asci were treated with lyticase and dissected using a micromanipulator
553 (Singer Instruments MSM 400) as previously described[5]. Spores were plated on YPD
554 agar and cultured at 30 °C, and germination was monitored for up to 7 days.
555 Resulting colonies were picked and stored in glycerol stocks until further analyses.

556 **Ascus micromanipulation and polyploid detection**

557 Complete asci, irrespective of spore number, were randomly isolated and plated
558 onto YPD agar using a micromanipulator (Singer Instruments MSM 400) and
559 incubated at 30 °C. After colony formation (approximately 2 days), a rapid
560 preliminary ploidy assessment was performed as described in the section Flow
561 cytometry. Colonies suspected to be polyploid were subsequently single-colony
562 streaked, and ploidy was validated by flow cytometry.

563 **Genomic DNA isolation**

564 Genomic DNA was extracted either using the E-Z 96 Tissue DNA Kit (Omega Bio-
565 Tek), following the manufacturer's instructions, or using the SDS-Kac protocol as
566 previously described[55].

567 **Genome sequencing and bioinformatic analysis**

568 Genomic DNA was sequenced using Illumina paired-end sequencing (2 × 150 bp)
569 with an average insert size of approximately 300 bp. Read quality was assessed
570 using FastQC (v0.12.1)[56] and summarized with MultiQC (v1.13)[57]. Read trimming
571 and filtering were performed using Trimmomatic (v0.39)[58], with parallel execution
572 managed using GNU Parallel (v20190322)[59].

573 Read alignment and variant calling were performed using a custom Snakemake-
574 based pipeline (https://github.com/CintiaG/poly_CCN_and_VC.git). Sequencing
575 reads were aligned to the reference genome using BWA (v0.7.18)[60]. SAM files were
576 converted to BAM format and sorted using SAMtools (v1.21)[61]. Duplicate reads were

identified and marked using GATK MarkDuplicatesSpark (v4.5.0.0)[62]. Variants were called per strain using GATK HaplotypeCaller in gVCF mode. Individual gVCF files were merged using GATK CombineGVCFs, and joint genotyping was performed with GATK GenotypeGVCFs to generate final VCF files.

Chromosome copy number (CCN) was estimated from sequencing depth using BEDTools (v2.29.2)[63]. CCN and segmental aneuploidies were inferred using in-house scripts (plot_depth.R and plot_copies.R; https://github.com/CintiaG/wgs-aneuploidy-abr.git).

Allele balance ratio (*ABR*) was calculated by extracting read depth (DP) and allele depth (AD) information from VCF files using BCFtools (v1.13)[64]. Text outputs were converted to fst format using the fst package (v0.9.8, http://www.fstpackage.org). *ABR* values were computed using the allele_balance_ratio.R script (https://github.com/CintiaG/wgs-aneuploidy-abr.git), retaining variants with *ABR* between 0.125 and 0.875. The number of heterozygous sites was estimated considering only variants with up to three alleles. In selected cases, CCN estimates were manually refined using *ABR* information, and genome-wide visualizations were generated using the plot_allele_balance_ratio.R script (https://github.com/CintiaG/wgs-aneuploidy-abr.git).

Data availability

The data for this study have been deposited in the European Nucleotide Archive (ENA) at EMBL-EBI under accession number PRJEB108394.

598 **References**

599

600 1. Morris, J. P., Baslan, T., Soltis, D. E., Soltis, P. S. & Fox, D. T. Integrating the
601 Study of Polyploidy Across Organisms, Tissues, and Disease. *Annu. Rev. Genet.* **58**,
602 297–318 (2024).
603 2. Fischer, G., Liti, G. & Llorente, B. The budding yeast life cycle: More complex
604 than anticipated? *Yeast Chichester Engl.* **38**, 5–11 (2021).
605 3. Selmecki, A. *et al.* Polyploidy can drive rapid adaptation in yeast. *Nature* **519**,
606 349–352 (2015).
607 4. Albertin, W. & Marullo, P. Polyploidy in fungi: evolution after whole-genome
608 duplication. *Proc. R. Soc. B Biol. Sci.* **279**, 2497–2509 (2012).
609 5. Vittorelli, N. *et al.* Repeated losses of self-fertility shaped heterozygosity and
610 polyploidy in yeast evolution. *Proc. Natl. Acad. Sci.* **123**, e2525679123 (2026).
611 6. Ward, C. M. *et al.* Recombination, admixture and genome instability shape
612 the genomic landscape of Saccharomyces cerevisiae derived from spontaneous
613 grape ferments. *PLOS Genet.* **20**, e1011223 (2024).
614 7. Peter, J. *et al.* Genome evolution across 1,011 Saccharomyces cerevisiae
615 isolates. *Nature* **556**, 339 (2018).
616 8. Duan, S.-F. *et al.* The origin and adaptive evolution of domesticated
617 populations of yeast from Far East Asia. *Nat. Commun.* **9**, 2690 (2018).
618 9. Loegler, V., Friedrich, A. & Schacherer, J. Overview of the Saccharomyces
619 cerevisiae population structure through the lens of 3,034 genomes. *G3 Bethesda Md*
620 **14**, jkae245 (2024).
621 10. Ezov, T. K. *et al.* Molecular-Genetic Biodiversity in a Natural Population of
622 the Yeast Saccharomyces cerevisiae From "Evolution Canyon": Microsatellite
623 Polymorphism, Ploidy and Controversial Sexual Status. *Genetics* **174**, 1455–1468
624 (2006).
625 11. Muller, L. A. H. & McCusker, J. H. Microsatellite analysis of genetic diversity
626 among clinical and nonclinical Saccharomyces cerevisiae isolates suggests
627 heterozygote advantage in clinical environments. *Mol. Ecol.* **18**, 2779–2786 (2009).

628 12. Segraves, K. A. & Anneberg, T. J. Species interactions and plant polyploidy.
629 *Am. J. Bot.* **103**, 1326–1335 (2016).
630 13. Wood, T. E. *et al.* The frequency of polyploid speciation in vascular plants.
631 *Proc. Natl. Acad. Sci.* **106**, 13875–13879 (2009).
632 14. MABLE, B. K. 'Why polyploidy is rarer in animals than in plants': myths and
633 mechanisms. *Biol. J. Linn. Soc.* **82**, 453–466 (2004).
634 15. Mable, B. K., Alexandrou, M. A. & Taylor, M. I. Genome duplication in
635 amphibians and fish: an extended synthesis. *J. Zool.* **284**, 151–182 (2011).
636 16. David, K. T. Global gradients in the distribution of animal polyploids. *Proc.*
637 *Natl. Acad. Sci. U. S. A.* **119**, e2214070119 (2022).
638 17. Mezzasalma, M., Brunelli, E., Odierna, G. & Guarino, F. M. Evolutionary and
639 Genomic Diversity of True Polyploidy in Tetrapods. *Anim. Open Access J. MDPI* **13**,
640 1033 (2023).
641 18. Bielski, C. M. *et al.* Genome doubling shapes the evolution and prognosis of
642 advanced cancers. *Nat. Genet.* **50**, 1189–1195 (2018).
643 19. Lambuta, R. A. *et al.* Whole-genome doubling drives oncogenic loss of
644 chromatin segregation. *Nature* **615**, 925–933 (2023).
645 20. Martínez-Jiménez, F. *et al.* Pan-cancer whole-genome comparison of primary
646 and metastatic solid tumours. *Nature* **618**, 333–341 (2023).
647 21. Otto, S. P. & Whitton, J. Polyploid incidence and evolution. *Annu. Rev. Genet.*
648 **34**, 401–437 (2000).
649 22. Ramsey, J. & Schemske, D. W. PATHWAYS, MECHANISMS, AND RATES
650 OF POLYPLOID FORMATION IN FLOWERING PLANTS. *Annu. Rev. Ecol. Evol.*
651 *Syst.* **29**, 467–501 (1998).
652 23. Pomper, S., Daniels, K. M. & McKee, D. W. Genetic Analysis of Polyploid
653 Yeast. *Genetics* **39**, 343–355 (1954).
654 24. Gunge, N. & Nakatomi, Y. Genetic Mechanisms of Rare Matings of the Yeast
655 SACCHAROMYCES CEREVISIAE Heterozygous for Mating Type. *Genetics* **70**, 41–
656 58 (1972).
657 25. Wolfe, K. H. & Shields, D. C. Molecular evidence for an ancient duplication
658 of the entire yeast genome. *Nature* **387**, 708–713 (1997).

659 26. Marcet-Houben, M. & Gabaldón, T. Beyond the Whole-Genome Duplication:
660 Phylogenetic Evidence for an Ancient Interspecies Hybridization in the Baker's
661 Yeast Lineage. *PLOS Biol.* **13**, e1002220 (2015).
662 27. Marsit, S., Hénault, M., Charron, G., Fijarczyk, A. & Landry, C. R. The neutral
663 rate of whole-genome duplication varies among yeast species and their hybrids. *Nat.*
664 *Commun.* **12**, 3126 (2021).
665 28. Charron, G., Marsit, S., Hénault, M., Martin, H. & Landry, C. R. Spontaneous
666 whole-genome duplication restores fertility in interspecific hybrids. *Nat. Commun.*
667 **10**, 1–10 (2019).
668 29. Tong, K. *et al.* Genome duplication in a long-term multicellularity evolution
669 experiment. *Nature* **639**, 691–699 (2025).
670 30. Mayer, V. W. & Aguilera, A. High levels of chromosome instability in
671 polyploids of Saccharomyces cerevisiae. *Mutat. Res.* **231**, 177–186 (1990).
672 31. Gerstein, A. C., Chun, H.-J. E., Grant, A. & Otto, S. P. Genomic convergence
673 toward diploidy in Saccharomyces cerevisiae. *PLoS Genet.* **2**, e145 (2006).
674 32. Gerstein, A. C., McBride, R. M. & Otto, S. P. Ploidy reduction in
675 Saccharomyces cerevisiae. *Biol. Lett.* **4**, 91–94 (2008).
676 33. Dutta, A., Dutreux, F. & Schacherer, J. Loss of Heterozygosity Spectrum
677 Depends on Ploidy Level in Natural Yeast Populations. *Mol. Biol. Evol.* **39**, msac214
678 (2022).
679 34. Fox, D. T. & Duronio, R. J. Endoreplication and polyploidy: insights into
680 development and disease. *Development* **140**, 3–12 (2013).
681 35. Edgar, B. A. & Orr-Weaver, T. L. Endoreplication Cell Cycles: More for Less.
682 *Cell* **105**, 297–306 (2001).
683 36. Harari, Y., Ram, Y., Rappoport, N., Hadany, L. & Kupiec, M. Spontaneous
684 Changes in Ploidy Are Common in Yeast. *Curr. Biol. CB* **28**, 825-835.e4 (2018).
685 37. De Chiara, M. *et al.* Domestication reprogrammed the budding yeast life
686 cycle. *Nat. Ecol. Evol.* **6**, 448–460 (2022).
687 38. Charles, J. St., Hamilton, M. L. & Petes, T. D. Meiotic Chromosome
688 Segregation in Triploid Strains of Saccharomyces cerevisiae. *Genetics* **186**, 537–550
689 (2010).

690 39. Mozzachiodi, S., Krogerus, K., Gibson, B., Nicolas, A. & Liti, G. Unlocking the
691 functional potential of polyploid yeasts. *Nat. Commun.* **13**, 2580 (2022).
692 40. Barrere, J., Nanda, P. & Murray, A. W. Alternating selection for dispersal and
693 multicellularity favors regulated life cycles. *Curr. Biol. CB* **33**, 1809-1817.e3 (2023).
694 41. Loidl, J. Meiotic chromosome pairing in triploid and tetraploid
695 Saccharomyces cerevisiae. *Genetics* **139**, 1511–1520 (1995).
696 42. Haber, J. E. BISEXUAL MATING BEHAVIOR IN A DIPLOID OF
697 SACCHAROMYCES CEREVISIAE: EVIDENCE FOR GENETICALLY
698 CONTROLLED NON-RANDOM CHROMOSOME LOSS DURING VEGETATIVE
699 GROWTH. *Genetics* **78**, 843–858 (1974).
700 43. Al Safadi, R., Weiss-Gayet, M., Briolay, J. & Aigle, M. A polyploid population
701 of Saccharomyces cerevisiae with separate sexes (dioecy). *FEMS Yeast Res.* **10**, 757–
702 768 (2010).
703 44. Pan, G., Zhou, Y., Fowke, L. C. & Wang, H. An efficient method for flow
704 cytometric analysis of pollen and detection of 2n nuclei in Brassica napus pollen.
705 *Plant Cell Rep.* **23**, 196–202 (2004).
706 45. Schild, D., Ananthaswamy, H. N. & Mortimer, R. K. An endomitotic effect of
707 a cell cycle mutation of Saccharomyces cerevisiae. *Genetics* **97**, 551–562 (1981).
708 46. Andreychuk, Y., Zhuk, A., Tarakhovskaya, E., Inge-Vechtomov, S. &
709 Stepchenkova, E. Rate of spontaneous polyploidization in haploid yeast
710 Saccharomyces cerevisiae. *Biol. Commun.* **67**, 88–96 (2022).
711 47. Tung, S., Bakerlee, C. W., Phillips, A. M., Nguyen Ba, A. N. & Desai, M. M.
712 The genetic basis of differential autodiploidization in evolving yeast populations.
713 *G3 GenesGenomesGenetics* **11**, jkab192 (2021).
714 48. Hose, J. *et al.* The genetic basis of aneuploidy tolerance in wild yeast. *eLife* **9**,
715 e52063 (2020).
716 49. Garrido, C. *et al.* Natural diversity of telomere length distributions across 100
717 Saccharomyces cerevisiae strains. *Genome Res.* gr.281132.125 (2026)
718 doi:10.1101/gr.281132.125.
719 50. Gómez-Muñoz, C. & Fischer, G. MuPETFlow: multiple ploidy estimation tool
720 from flow cytometry data. *BMC Genomics* **26**, 301 (2025).

721 51. Cubillos, F. A., Louis, E. J. & Liti, G. Generation of a large set of genetically
722 tractable haploid and diploid Saccharomyces strains. *FEMS Yeast Res.* **9**, 1217–1225
723 (2009).
724 52. Huxley, C., Green, E. D. & Dunham, I. Rapid assessment of S. cerevisiae
725 mating type by PCR. *Trends Genet. TIG* **6**, 236 (1990).
726 53. Arras, S. D. M. *et al.* Creeping yeast: a simple, cheap and robust protocol for
727 the identification of mating type in Saccharomyces cerevisiae. *FEMS Yeast Res.* **22**,
728 foac017 (2022).
729 54. de Barros Lopes, M., Bellon, J. R., Shirley, N. J. & Ganter, P. F. Evidence for
730 multiple interspecific hybridization in *Saccharomyces* sensu stricto species. *FEMS*
731 *Yeast Res.* **1**, 323–331 (2002).
732 55. Agier, N. *et al.* A transient mutational burst occurs during yeast colony
733 development. *Mol. Syst. Biol.* **21**, 1214–1236 (2025).
734 56. Andrews, S. (2010) FastQC A Quality Control Tool for High Throughput
735 Sequence Data. - References - Scientific Research Publishing.
736 https://www.scirp.org/reference/referencespapers?referenceid=2781642.
737 57. Ewels, P., Magnusson, M., Lundin, S. & Käller, M. MultiQC: summarize
738 analysis results for multiple tools and samples in a single report. *Bioinforma. Oxf.*
739 *Engl.* **32**, 3047–3048 (2016).
740 58. Bolger, A. M., Lohse, M. & Usadel, B. Trimmomatic: a flexible trimmer for
741 Illumina sequence data. *Bioinforma. Oxf. Engl.* **30**, 2114–2120 (2014).
742 59. GNU Parallel 2018. *Guide books*
743 https://dl.acm.org/doi/abs/10.5555/3235180 doi:10.5555/3235180.
744 60. Li, H. & Durbin, R. Fast and accurate short read alignment with Burrows–
745 Wheeler transform. *Bioinformatics* **25**, 1754–1760 (2009).
746 61. Li, H. *et al.* The Sequence Alignment/Map format and SAMtools. *Bioinforma.*
747 *Oxf. Engl.* **25**, 2078–2079 (2009).
748 62. Van der Auwera, G. A. *et al.* From FastQ data to high confidence variant calls:
749 the Genome Analysis Toolkit best practices pipeline. *Curr. Protoc. Bioinforma.* **43**,
750 11.10.1-11.10.33 (2013).

751 63. Quinlan, A. R. & Hall, I. M. BEDTools: a flexible suite of utilities for
752 comparing genomic features. *Bioinforma. Oxf. Engl.* **26**, 841–842 (2010).
753 64. Danecek, P. & McCarthy, S. A. BCFtools/csq: haplotype-aware variant
754 consequences. *Bioinformatics* **33**, 2037–2039 (2017).
755

756